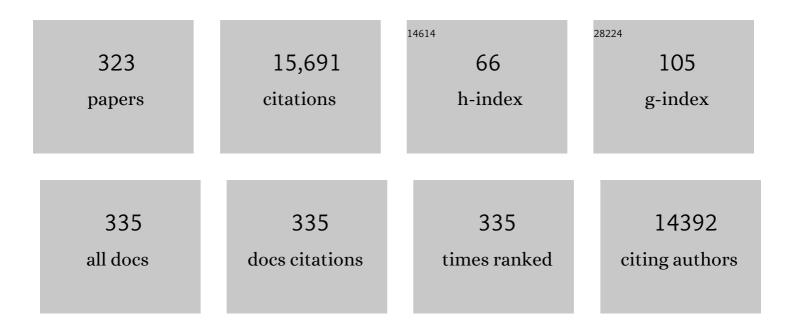
List of Publications by Year in descending order

Source: https://exaly.com/author-pdf/2526899/publications.pdf Version: 2024-02-01



<u>\/ГГСни</u>

#	Article	IF	CITATIONS
1	Degradation of atrazine by cobalt-mediated activation of peroxymonosulfate: Different cobalt counteranions in homogenous process and cobalt oxide catalysts in photolytic heterogeneous process. Water Research, 2009, 43, 2513-2521.	5.3	391
2	The Aqueous Degradation of Butylated Hydroxyanisole by UV/S2O82-: Study of Reaction Mechanisms via Dimerization and Mineralization. Environmental Science & amp; Technology, 2007, 41, 613-619.	4.6	390
3	Facile Route for Synthesizing Ordered Mesoporous Ni–Ce–Al Oxide Materials and Their Catalytic Performance for Methane Dry Reforming to Hydrogen and Syngas. ACS Catalysis, 2013, 3, 1638-1651.	5.5	362
4	Degradation of carbamazepine by Fe(II)-activated persulfate process. Journal of Hazardous Materials, 2014, 268, 23-32.	6.5	314
5	Quantitative prediction of direct and indirect dye ozonation kinetics. Water Research, 2000, 34, 3153-3160.	5.3	243
6	Environmental application of graphene-based CoFe2O4 as an activator of peroxymonosulfate for the degradation of a plasticizer. Chemical Engineering Journal, 2015, 263, 435-443.	6.6	238
7	Modeling the heterogeneous peroxymonosulfate/Co-MCM41 process for the degradation of caffeine and the study of influence of cobalt sources. Chemical Engineering Journal, 2014, 235, 10-18.	6.6	218
8	Degradation of benzotriazole by a novel Fenton-like reaction with mesoporous Cu/MnO 2 : Combination of adsorption and catalysis oxidation. Applied Catalysis B: Environmental, 2016, 199, 447-457.	10.8	206
9	Dye Removal from Textile Dye Wastewater Using Recycled Alum Sludge. Water Research, 2001, 35, 3147-3152.	5.3	201
10	Enhanced photocatalytic degradation of ciprofloxacin over Bi2O3/(BiO)2CO3 heterojunctions: Efficiency, kinetics, pathways, mechanisms and toxicity evaluation. Chemical Engineering Journal, 2018, 334, 453-461.	6.6	198
11	The direct photolysis and photocatalytic degradation of alachlor at different TiO2 and UV sources. Chemosphere, 2003, 50, 981-987.	4.2	179
12	Coupling metal–organic frameworks and g-CN to derive Fe@N-doped graphene-like carbon for peroxymonosulfate activation: Upgrading framework stability and performance. Applied Catalysis B: Environmental, 2019, 255, 117763.	10.8	175
13	Crystal-plane effect of nanoscale CeO ₂ on the catalytic performance of Ni/CeO ₂ catalysts for methane dry reforming. Catalysis Science and Technology, 2016, 6, 3594-3605.	2.1	170
14	The Hydrogen Peroxide-Assisted Photocatalytic Degradation of Alachlor in TiO2Suspensions. Environmental Science & Technology, 2003, 37, 2310-2316.	4.6	166
15	Degradation of a xanthene dye by Fe(II)-mediated activation of Oxone process. Journal of Hazardous Materials, 2011, 186, 1455-1461.	6.5	159
16	Catalytic degradation of caffeine in aqueous solutions by cobalt-MCM41 activation of peroxymonosulfate. Applied Catalysis B: Environmental, 2013, 134-135, 324-332.	10.8	150
17	The effect of solution pH and peroxide in the TiO2-induced photocatalysis of chlorinated aniline. Journal of Hazardous Materials, 2007, 141, 86-91.	6.5	149
18	Glowâ€Discharge Plasmaâ€Assisted Design of Cobalt Catalysts for Fischer–Tropsch Synthesis. Angewandte Chemie - International Edition, 2008, 47, 5052-5055.	7.2	149

#	Article	IF	CITATIONS
19	Crossâ€Coupled Macroâ€Mesoporous Carbon Network toward Record High Energyâ€Power Density Supercapacitor at 4 V. Advanced Functional Materials, 2018, 28, 1806153.	7.8	145
20	Nanoscaled magnetic CuFe2O4 as an activator of peroxymonosulfate for the degradation of antibiotics norfloxacin. Separation and Purification Technology, 2019, 212, 536-544.	3.9	141
21	Simultaneous adsorption of Cr(VI) and phenol by biochar-based iron oxide composites in water: Performance, kinetics and mechanism. Journal of Hazardous Materials, 2021, 416, 125930.	6.5	138
22	Modeling the reaction kinetics of Fenton's process on the removal of atrazine. Chemosphere, 2003, 51, 305-311.	4.2	137
23	Degradation of 2,4,5-trichlorophenoxyacetic acid by a novel Electro-Fe(II)/Oxone process using iron sheet as the sacrificial anode. Water Research, 2011, 45, 3883-3889.	5.3	137
24	Hybrid porous magnetic bentonite-chitosan beads for selective removal of radioactive cesium in water. Journal of Hazardous Materials, 2019, 362, 160-169.	6.5	135
25	Sulfate radical-based photo-Fenton reaction derived by CuBi 2 O 4 and its composites with α-Bi 2 O 3 under visible light irradiation: Catalyst fabrication, performance and reaction mechanism. Applied Catalysis B: Environmental, 2018, 235, 264-273.	10.8	133
26	A review on the bioenergetics of anaerobic microbial metabolism close to the thermodynamic limits and its implications for digestion applications. Bioresource Technology, 2018, 247, 1095-1106.	4.8	133
27	Novel carbon based Fe-Co oxides derived from Prussian blue analogues activating peroxymonosulfate: Refractory drugs degradation without metal leaching. Chemical Engineering Journal, 2020, 379, 122274.	6.6	133
28	The mechanism of the surfactant-aided soil washing system for hydrophobic and partial hydrophobic organics. Science of the Total Environment, 2003, 307, 83-92.	3.9	129
29	Photocatalytic degradation and decomposition mechanism of fluoroquinolones norfloxacin over bismuth tungstate: Experiment and mathematic model. Applied Catalysis B: Environmental, 2015, 168-169, 175-182.	10.8	126
30	Transition metal-embedded two-dimensional C ₃ N as a highly active electrocatalyst for oxygen evolution and reduction reactions. Journal of Materials Chemistry A, 2019, 7, 12050-12059.	5.2	123
31	The degradation of endocrine disruptor di-n-butyl phthalate by UV irradiation: A photolysis and product study. Chemosphere, 2005, 60, 1045-1053.	4.2	119
32	Degradation of antibiotic norfloxacin in aqueous solution by visible-light-mediated C-TiO2 photocatalysis. Journal of Hazardous Materials, 2012, 219-220, 183-189.	6.5	118
33	Environmental Remediation Applications of Carbon Nanotubes and Graphene Oxide: Adsorption and Catalysis. Nanomaterials, 2019, 9, 439.	1.9	117
34	The photocatalytic degradation of dicamba in TiO2 suspensions with the help of hydrogen peroxide by different near UV irradiations. Water Research, 2004, 38, 1037-1043.	5.3	115
35	Modeling the quantum yields of herbicide 2,4-D decay in UV/H2O2 process. Chemosphere, 2001, 44, 935-941.	4.2	113
36	Synergistic oxidation of Bisphenol A in a heterogeneous ultrasound-enhanced sludge biochar catalyst/persulfate process: Reactivity and mechanism. Journal of Hazardous Materials, 2020, 384, 121385.	6.5	110

#	Article	IF	CITATIONS
37	Remediation of contaminated soil by a solvent/surfactant system. Chemosphere, 2003, 53, 9-15.	4.2	105
38	UiO-66-NH2/GO Composite: Synthesis, Characterization and CO2 Adsorption Performance. Materials, 2018, 11, 589.	1.3	105
39	Visible light photocatalytic degradation of tetracycline with porous Ag/graphite carbon nitride plasmonic composite: Degradation pathways and mechanism. Journal of Colloid and Interface Science, 2020, 574, 110-121.	5.0	105
40	Highâ€Density and Thermally Stable Palladium Singleâ€Atom Catalysts for Chemoselective Hydrogenations. Angewandte Chemie - International Edition, 2020, 59, 21613-21619.	7.2	103
41	Ozonation of phenacetin in associated with a magnetic catalyst CuFe2O4: The reaction and transformation. Chemical Engineering Journal, 2015, 262, 552-562.	6.6	102
42	Lead metal removal by recycled alum sludge. Water Research, 1999, 33, 3019-3025.	5.3	99
43	Preparation and characterization of a plasma treated NiMgSBA-15 catalyst for methane reforming with CO2 to produce syngas. Catalysis Science and Technology, 2013, 3, 2278.	2.1	94
44	Determination and toxicity evaluation of the generated products in sulfamethoxazole degradation by UV/CoFe 2 O 4 /TiO 2. Journal of Hazardous Materials, 2016, 314, 197-203.	6.5	94
45	Strategies to extend near-infrared light harvest of polymer carbon nitride photocatalysts. Coordination Chemistry Reviews, 2021, 439, 213947.	9.5	94
46	Self-Propagated Flaming Synthesis of Highly Active Layered CuO-δ-MnO ₂ Hybrid Composites for Catalytic Total Oxidation of Toluene Pollutant. ACS Applied Materials & Interfaces, 2017, 9, 21798-21808.	4.0	91
47	The nature of cobalt species in carbon nanotubes and their catalytic performance in Fischer–Tropsch reaction. Journal of Materials Chemistry, 2009, 19, 9241.	6.7	88
48	Nearâ€Infrared Light Responsive TiO ₂ for Efficient Solar Energy Utilization. Advanced Functional Materials, 2022, 32, .	7.8	88
49	Photodechlorination of Polychlorobenzene Congeners in Surfactant Micelle Solutions. Environmental Science & Technology, 1994, 28, 2415-2422.	4.6	83
50	Heterogeneous Lollipop-like V ₂ O ₅ /ZnO Array: A Promising Composite Nanostructure for Visible Light Photocatalysis. Langmuir, 2010, 26, 11615-11620.	1.6	83
51	Novel CuCo ₂ O ₄ Composite Spinel with a Meso-Macroporous Nanosheet Structure for Sulfate Radical Formation and Benzophenone-4 Degradation: Interface Reaction, Degradation Pathway, and DFT Calculation. ACS Applied Materials & amp; Interfaces, 2020, 12, 20522-20535.	4.0	83
52	Photodegradation of 4-chlorophenoxyacetic acid under visible LED activated N-doped TiO 2 and the mechanism of stepwise rate increment of the reused catalyst. Journal of Hazardous Materials, 2017, 338, 491-501.	6.5	80
53	Photodechlorination Mechanism of DDT in a UV/Surfactant System. Environmental Science & Technology, 1999, 33, 421-425.	4.6	79
54	Photodegradation of 2,4-dichlorophenoxyacetic acid in various iron-mediated oxidation systems. Water Research, 2003, 37, 4405-4412.	5.3	79

#	Article	IF	CITATIONS
55	Photo-assisted degradation of 2,4,5-trichlorophenoxyacetic acid by Fe(II)-catalyzed activation of Oxone process: The role of UV irradiation, reaction mechanism and mineralization. Applied Catalysis B: Environmental, 2012, 123-124, 151-161.	10.8	76
56	Low-temperature catalytic combustion of methane over MnO x –CeO2 mixed oxide catalysts: Effect of preparation method. Catalysis Letters, 2007, 113, 59-64.	1.4	73
57	Degradation of iopromide by combined UV irradiation and peroxydisulfate. Journal of Hazardous Materials, 2010, 181, 508-513.	6.5	73
58	Experimental and Modeling Study of Methane Adsorption on Activated Carbon Derived from Anthracite. Journal of Chemical & Engineering Data, 2011, 56, 4919-4926.	1.0	72
59	Effects of Combined and Sequential Addition of Dual Oxidants (H2O2/S2O82-) on the Aqueous Carbofuran Photodegradation. Journal of Agricultural and Food Chemistry, 2006, 54, 10047-10052.	2.4	71
60	Diphenamid degradation via sulfite activation under visible LED using Fe (III) impregnated N-doped TiO2 photocatalyst. Applied Catalysis B: Environmental, 2019, 244, 823-835.	10.8	71
61	Synergy of sulfate and hydroxyl radicals in UV/S2O82â ^{~/} /H2O2 oxidation of iodinated X-ray contrast medium iopromide. Chemical Engineering Journal, 2011, 178, 154-160.	6.6	70
62	Remediation of Contaminated Soils by Surfactant-Aided Soil Washing. Practice Periodical of Hazardous, Toxic and Radioactive Waste Management, 2003, 7, 19-24.	0.4	69
63	In Situ Coprecipitation Formed Highly Water-Dispersible Magnetic Chitosan Nanopowder for Removal of Heavy Metals and Its Adsorption Mechanism. ACS Sustainable Chemistry and Engineering, 2018, 6, 16754-16765.	3.2	68
64	Efficient Degradation of an Antibiotic Norfloxacin in Aqueous Solution via a Simulated Solar-Light-Mediated Bi ₂ WO ₆ Process. Industrial & Engineering Chemistry Research, 2012, 51, 4887-4893.	1.8	67
65	Self-assembled Ni/NiO/RGO heterostructures for high-performance supercapacitors. RSC Advances, 2015, 5, 77958-77964.	1.7	67
66	Removal of herbicide atrazine by a novel biochar based iron composite coupling with peroxymonosulfate process from soil: Synergistic effect and mechanism. Chemical Engineering Journal, 2021, 409, 127684.	6.6	67
67	Comparison of phenacetin degradation in aqueous solutions by catalytic ozonation with CuFe 2 O 4 and its precursor: Surface properties, intermediates and reaction mechanisms. Chemical Engineering Journal, 2016, 284, 28-36.	6.6	66
68	Strategic combination of nitrogen-doped carbon quantum dots and g-C3N4: Efficient photocatalytic peroxydisulfate for the degradation of tetracycline hydrochloride and mechanism insight. Separation and Purification Technology, 2021, 272, 118947.	3.9	65
69	A study of kinetic modelling and reaction pathway of 2,4-dichlorophenol transformation by photo-fenton-like oxidation. Journal of Hazardous Materials, 2005, 121, 119-126.	6.5	64
70	A systematic study of the degradation of dimethyl phthalate using a high-frequency ultrasonic process. Ultrasonics Sonochemistry, 2013, 20, 892-899.	3.8	64
71	The role of organic ligands in ferrous-induced photochemical degradation of 2,4-dichlorophenoxyacetic acid. Chemosphere, 2007, 67, 1601-1611.	4.2	63
72	Removals of Cr(VI) and Cd(II) by a novel nanoscale zero valent iron/peroxydisulfate process and its Fenton-like oxidation of pesticide atrazine: Coexisting effect, products and mechanism. Chemical Engineering Journal, 2020, 397, 125382.	6.6	63

#	Article	IF	CITATIONS
73	Magnetically recyclable hollow Co–B nanospindles as catalysts for hydrogen generation from ammonia borane. Journal of Materials Science, 2010, 45, 2862-2867.	1.7	62
74	Reaction Mechanism of Linuron Degradation in TiO ₂ Suspension under Visible Light Irradiation with the Assistance of H ₂ O ₂ . Environmental Science & Technology, 2009, 43, 6183-6189.	4.6	61
75	In situ controllable assembly of layered-double-hydroxide-based nickel nanocatalysts for carbon dioxide reforming of methane. Catalysis Science and Technology, 2015, 5, 1588-1597.	2.1	60
76	FeS2 assisted degradation of atrazine by bentonite-supported nZVI coupling with hydrogen peroxide process in water: Performance and mechanism. Science of the Total Environment, 2021, 754, 142155.	3.9	60
77	Photo-sensitization of diazo disperse dye in aqueous acetone. Chemosphere, 1999, 39, 1667-1677.	4.2	59
78	Photocatalytic oxidation of carbamazepine in triclinic-WO3 suspension: Role of alcohol and sulfate radicals in the degradation pathway. Applied Catalysis A: General, 2013, 468, 240-249.	2.2	58
79	Heterogeneous catalytic ozonation of phenacetin in water using magnetic spinel ferrite as catalyst: Comparison of surface property and efficiency. Journal of Molecular Catalysis A, 2015, 396, 164-173.	4.8	58
80	Degradation of 2,4-dichlorophenol by a novel iron based system and its synergism with Cd(II) immobilization in a contaminated soil. Chemical Engineering Journal, 2020, 379, 122313.	6.6	58
81	Phototransformations of Polychlorobiphenyls in Brij 58 Micellar Solutions. Environmental Science & Technology, 1998, 32, 1989-1993.	4.6	56
82	Model applications and mechanism study on the degradation of atrazine by Fenton's system. Journal of Hazardous Materials, 2005, 118, 227-237.	6.5	56
83	A study of the reaction mechanisms of the degradation of 2,4-dichlorophenoxyacetic acid by oxalate-mediated photooxidation. Water Research, 2004, 38, 4213-4221.	5.3	55
84	Ultrasound-assisted heterogeneous activation of peroxymonosulphate by natural pyrite for 2,4-diclorophenol degradation in water: Synergistic effects, pathway and mechanism. Chemical Engineering Journal, 2020, 389, 123771.	6.6	55
85	The prediction of partitioning coefficients for chemicals causing environmental concern. Science of the Total Environment, 2000, 248, 1-10.	3.9	54
86	H2O2 assisted degradation of antibiotic norfloxacin over simulated solar light mediated Bi2WO6: Kinetics and reaction pathway. Chemical Engineering Journal, 2016, 296, 310-318.	6.6	53
87	S-doped TiO2 photocatalyst for visible LED mediated oxone activation: Kinetics and mechanism study for the photocatalytic degradation of pyrimethanil fungicide. Chemical Engineering Journal, 2021, 411, 128450.	6.6	53
88	Mesoporous Ni/Ce _{1â^x} Ni _x O _{2â^y} heterostructure as an efficient catalyst for converting greenhouse gas to H ₂ and syngas. Catalysis Science and Technology, 2016, 6, 851-862.	2.1	52
89	Novel highly porous magnetic hydrogel beads composed of chitosan and sodium citrate: an effective adsorbent for the removal of heavy metals from aqueous solutions. Environmental Science and Pollution Research, 2017, 24, 16520-16530.	2.7	52
90	Degradation of atrazine by modified stepwise-Fenton's processes. Chemosphere, 2007, 67, 755-761.	4.2	51

#	Article	IF	CITATIONS
91	Phosgene-Free Synthesis of Phenyl Isocyanate by Catalytic Decomposition of Methyl N-Phenyl Carbamate over Bi2O3 Catalyst. Catalysis Letters, 2008, 123, 307-316.	1.4	51
92	Facile synthesis of homogeneous hollow microsphere Cu–Mn based catalysts for catalytic oxidation of toluene. Chemosphere, 2020, 247, 125812.	4.2	50
93	Recent advances in single-atom electrocatalysts supported on two-dimensional materials for the oxygen evolution reaction. Journal of Materials Chemistry A, 2021, 9, 9979-9999.	5.2	50
94	Observations of 2,4,6-trichlorophenol degradation by ozone. Chemosphere, 2003, 51, 237-243.	4.2	49
95	Promotion Effects of Platinum and Ruthenium on Carbon Nanotube Supported Cobalt Catalysts for Fischer–Tropsch Synthesis. Catalysis Letters, 2011, 141, 438-444.	1.4	49
96	Defect engineering in polymeric carbon nitride photocatalyst: Synthesis, properties and characterizations. Advances in Colloid and Interface Science, 2021, 296, 102523.	7.0	49
97	Modeling the two stages of surfactant-aided soil washing. Water Research, 2001, 35, 761-767.	5.3	48
98	Degradation of the endocrine disruptor carbofuran by UV, O3 and O3/UV. Water Science and Technology, 2007, 55, 275-280.	1.2	47
99	Linuron decomposition in aqueous semiconductor suspension under visible light irradiation with and without H2O2. Chemical Engineering Journal, 2010, 158, 181-187.	6.6	47
100	Efficient degradation, mineralization and toxicity reduction of sulfamethoxazole under photo-activation of peroxymonosulfate by ferrate (VI). Chemical Engineering Journal, 2020, 389, 124084.	6.6	47
101	Sonophotolytic degradation of dimethyl phthalate without catalyst: Analysis of the synergistic effect and modeling. Water Research, 2013, 47, 1996-2004.	5.3	46
102	Degradation of di-n-butyl phthalate by a homogeneous sono–photo–Fenton process with in situ generated hydrogen peroxide. Chemical Engineering Journal, 2014, 240, 541-547.	6.6	46
103	Implication of iron nitride species to enhance the catalytic activity and stability of carbon nanotubes supported Fe catalysts for carbon-free hydrogen production <i>via</i> low-temperature ammonia decomposition. Catalysis Science and Technology, 2018, 8, 907-915.	2.1	46
104	Application of Fourier transform ion cyclotron resonance mass spectrometry to characterize natural organic matter. Chemosphere, 2020, 260, 127458.	4.2	46
105	Adsorption and Removal of a Xanthene Dye from Aqueous Solution Using Two Solid Wastes as Adsorbents. Industrial & Engineering Chemistry Research, 2011, 50, 8734-8741.	1.8	45
106	Hydrogen Production by Ethanol Steam Reforming on NiCuMgAl Catalysts Derived from Hydrotalcite-Like Precursors. Catalysis Letters, 2011, 141, 1228-1236.	1.4	45
107	Photocatalytic oxidation of monuron in the suspension of WO3 under the irradiation of UV–visible light. Chemosphere, 2012, 86, 1079-1086.	4.2	45
108	Regulation of Ni–CNT Interaction on Mn-Promoted Nickel Nanocatalysts Supported on Oxygenated CNTs for CO ₂ Selective Hydrogenation. ACS Applied Materials & Interfaces, 2018, 10, 41224-41236.	4.0	45

Wеі Сни

#	Article	IF	CITATIONS
109	Ibuprofen degradation and toxicity evolution during Fe2+/Oxone/UV process. Chemosphere, 2017, 167, 415-421.	4.2	44
110	Flexible metal-templated fabrication of mesoporous onion-like carbon and Fe ₂ O ₃ @N-doped carbon foam for electrochemical energy storage. Journal of Materials Chemistry A, 2018, 6, 13012-13020.	5.2	44
111	Microwave-Assisted Synthesis of NiCo2O4 Double-Shelled Hollow Spheres for High-Performance Sodium Ion Batteries. Nano-Micro Letters, 2018, 10, 13.	14.4	44
112	Application of ultrasonic wave to clean the surface of the TiO2 nanotubes prepared by the electrochemical anodization. Applied Surface Science, 2011, 257, 8478-8480.	3.1	43
113	Acceleration and Quenching of the Photolysis of PCB in the Presence of Surfactant and Humic Materials. Environmental Science & Technology, 2005, 39, 9211-9216.	4.6	42
114	A systematic study on photocatalysis of antipyrine: Catalyst characterization, parameter optimization, reaction mechanism and toxicity evolution to plankton. Water Research, 2017, 112, 167-175.	5.3	42
115	An unconventional approach to studying the reaction kinetics of the Fenton's oxidation of 2,4-dichlorophenoxyacetic acid. Chemosphere, 2004, 57, 1165-1171.	4.2	41
116	A new approach to quantify the degradation kinetics of linuron with UV, ozonation and UV/O3 processes. Chemosphere, 2009, 74, 1444-1449.	4.2	41
117	Atrazine degradation using chemical-free process of USUV: Analysis of the micro-heterogeneous environments and the degradation mechanisms. Journal of Hazardous Materials, 2014, 275, 166-174.	6.5	41
118	UV/ peroxymonosulfate process for degradation of chloral hydrate: Pathway and the role of radicals. Journal of Hazardous Materials, 2021, 401, 123837.	6.5	41
119	Mesoporous Co–B–N–H nanowires: superior catalysts for decomposition of hydrous hydrazine to generate hydrogen. Catalysis Science and Technology, 2014, 4, 3168.	2.1	40
120	Solar photocatalytic degradation of ibuprofen with a magnetic catalyst: Effects of parameters, efficiency in effluent, mechanism and toxicity evolution. Environmental Pollution, 2021, 276, 116691.	3.7	40
121	Synthesis, characterization and capacitive performance of hydrous manganese dioxide nanostructures. Nanotechnology, 2011, 22, 125703.	1.3	39
122	Modeling the ozonation of 2,4-dichlorophoxyacetic acid through a kinetic approach. Water Research, 2003, 37, 39-46.	5.3	38
123	Reaction pathways and kinetics of butylated hydroxyanisole with UV, ozonation, and UV/O3 processes. Water Research, 2007, 41, 765-774.	5.3	38
124	Oneâ€pot Synthesis of Ordered Mesoporous NiCeAl Oxide Catalysts and a Study of Their Performance in Methane Dry Reforming. ChemCatChem, 2014, 6, 1470-1480.	1.8	38
125	Monuron photodegradation using peroxymonosulfate activated by non-metal-doped TiO2 under visible LED and the modeling via a parallel-serial kinetic approach. Chemical Engineering Journal, 2018, 338, 411-421.	6.6	38
126	Formation and interdependence of disinfection byproducts during chlorination of natural organic matter in a conventional drinking water treatment plant. Chemosphere, 2020, 242, 125227.	4.2	38

#	Article	IF	CITATIONS
127	Facile synthesis of high-surface-area activated carbon from coal for supercapacitors and high CO ₂ sorption. RSC Advances, 2016, 6, 42019-42028.	1.7	37
128	Mechanism of enhanced diclofenac mineralization by catalytic ozonation over iron silicate-loaded pumice. Separation and Purification Technology, 2017, 173, 55-62.	3.9	37
129	Prediction of carbofuran degradation based on the hydroxyl radical's generation using the FeIII impregnated N doped-TiO2/H2O2/visible LED photo-Fenton-like process. Chemical Engineering Journal, 2020, 382, 122930.	6.6	37
130	Removal of antibiotics sulfadiazine by a biochar based material activated persulfate oxidation system: Performance, products and mechanism. Chemical Engineering Research and Design, 2022, 157, 411-419.	2.7	37
131	Biosourced Foamâ€Like Activated Carbon Materials as Highâ€Performance Supercapacitors. Advanced Sustainable Systems, 2018, 2, 1700123.	2.7	36
132	An Efficient Photocatalyst for Fast Reduction of Cr(VI) by Ultra-Trace Silver Enhanced Titania in Aqueous Solution. Catalysts, 2018, 8, 251.	1.6	36
133	Probing the enhanced catalytic activity of carbon nanotube supported Ni-LaO _x hybrids for the CO ₂ reduction reaction. Nanoscale, 2018, 10, 14207-14219.	2.8	36
134	Treatment of trichlorophenol by catalytic oxidation process. Water Research, 2003, 37, 2339-2346.	5.3	35
135	Cerium Promoted Nano Nickel Catalysts Ni-Ce/CNTs and Ni-Ce/Al ₂ O ₃ for CO ₂ Methanation. Integrated Ferroelectrics, 2014, 151, 116-125.	0.3	35
136	Plasma-Treated Bimetallic Ni–Pt Catalysts Derived from Hydrotalcites for the Carbon Dioxide Reforming of Methane. Catalysis Letters, 2014, 144, 293-300.	1.4	35
137	Sonophotolytic degradation of phthalate acid esters in water and wastewater: Influence of compound properties and degradation mechanisms. Journal of Hazardous Materials, 2015, 288, 43-50.	6.5	35
138	<scp>PAA</scp> /alumina composites prepared with different molecular weight polymers and utilized as support for nickelâ€based catalyst. Advances in Polymer Technology, 2018, 37, 2325-2335.	0.8	35
139	Tuning the Chemical Properties of Co–Ti ₃ C ₂ T <i>_x</i> MXene Materials for Catalytic CO ₂ Reduction. Small, 2021, 17, e2007509.	5.2	35
140	Atrazine removal by catalytic oxidation processes with or without UV irradiation. Applied Catalysis B: Environmental, 2005, 58, 165-174.	10.8	34
141	Effect of humic acid on the photolysis of the pesticide atrazine in a surfactant-aided soil-washing system in acidic condition. Water Research, 2005, 39, 2154-2166.	5.3	34
142	Degradation of methotrexate by UV/peroxymonosulfate: Kinetics, effect of operational parameters and mechanism. Chinese Journal of Chemical Engineering, 2020, 28, 2658-2667.	1.7	34
143	Effect of a second metal (Co, Cu, Mn or Zr) on nickel catalysts derived from hydrotalcites for the carbon dioxide reforming of methane. RSC Advances, 2016, 6, 70537-70546.	1.7	33
144	Various Metals (Ce, In, La, and Fe) Promoted Pt/Sn-SBA-15 as Highly Stable Catalysts for Propane Dehydrogenation. Industrial & Engineering Chemistry Research, 2019, 58, 10804-10818.	1.8	33

#	Article	IF	CITATIONS
145	Controlling oxygen vacancies of CoMn2O4 by loading on planar and tubular clay minerals and its application for boosted PMS activation. Journal of Hazardous Materials, 2022, 436, 129060.	6.5	33
146	Quantum yield study of the photodegradation of hydrophobic dyes in the presence of acetone sensitizer. Chemosphere, 2001, 44, 17-22.	4.2	32
147	Efficient activation of oxone by pyrite for the degradation of propanil: Kinetics and degradation pathway. Journal of Hazardous Materials, 2021, 403, 123930.	6.5	32
148	Ultrasound-assisted catalytic reduction of Cr(VI) by an acid mine drainage based nZVI coupling with FeS2 system from aqueous solutions: Performance and mechanism. Journal of Environmental Management, 2021, 278, 111518.	3.8	32
149	Peroxymonosulfate-assisted photocatalytic degradation of antibiotic norfloxacin by a calcium-based Ag3PO4 composite in water: Reactivity, products and mechanism. Journal of Cleaner Production, 2022, 330, 129806.	4.6	32
150	Photodegradation of Sulfamethoxazole with a Recyclable Catalyst. Industrial & Engineering Chemistry Research, 2015, 54, 12763-12769.	1.8	31
151	Carbon Nanotubes Supported Nickel as the Highly Efficient Catalyst for Hydrogen Production through Glycerol Steam Reforming. ACS Sustainable Chemistry and Engineering, 2018, 6, 14403-14413.	3.2	31
152	Computational screening of transition metal-doped phthalocyanine monolayers for oxygen evolution and reduction. Nanoscale Advances, 2020, 2, 710-716.	2.2	30
153	Remarkable Promotion of Benzene Formation in Methane Aromatization with Ethane Addition. Topics in Catalysis, 2003, 22, 131-134.	1.3	29
154	The dose and ratio effects of Fe(II) and H ₂ O ₂ in Fenton's process on the removal of atrazine. Environmental Technology (United Kingdom), 2003, 24, 703-710.	1.2	29
155	Naphthalene degradation by Fe2+/Oxone/UV – Applying an unconventional kinetics model and studying the reaction mechanism. Chemosphere, 2019, 218, 110-118.	4.2	29
156	Spectral and mass spectrometric characteristics of different molecular weight fractions of dissolved organic matter. Separation and Purification Technology, 2020, 253, 117390.	3.9	29
157	Modeling of photodecoloration of azo dye in a cocktail photolysis system. Water Research, 2002, 36, 3350-3358.	5.3	28
158	Destruction ofo-Chloroaniline in UV/TiO2Reaction with Photosensitizing Additives. Industrial & Engineering Chemistry Research, 2005, 44, 8184-8189.	1.8	28
159	The use of oxyhalogen in photocatalytic reaction to remove o-chloroaniline in TiO2 dispersion. Chemosphere, 2007, 66, 2106-2113.	4.2	28
160	Pd nanoparticles immobilized on carbon nanotubes with a polyaniline coaxial coating for the Heck reaction: coating thickness as the key factor influencing the efficiency and stability of the catalyst. Catalysis Science and Technology, 2018, 8, 1423-1434.	2.1	28
161	Cooperation of multi-walled carbon nanotubes and cobalt doped TiO2 to activate peroxymonosulfate for antipyrine photocatalytic degradation. Separation and Purification Technology, 2022, 282, 119996.	3.9	28
162	Reaction kinetics of UV-decolourization for dye materials. Chemosphere, 1998, 37, 961-974.	4.2	27

#	Article	IF	CITATIONS
163	Promotion Effect of CaO Modification on Mesoporous Al ₂ O ₃ -Supported Ni Catalysts for CO ₂ Methanation. International Journal of Chemical Engineering, 2016, 2016, 1-7.	1.4	27
164	Physicochemical Studies of Adsorptive Denitrogenation by Oxidized Activated Carbons. Industrial & amp; Engineering Chemistry Research, 2017, 56, 5033-5041.	1.8	27
165	Transition-metal single atoms embedded into defective BC ₃ as efficient electrocatalysts for oxygen evolution and reduction reactions. Nanoscale, 2021, 13, 1331-1339.	2.8	27
166	Peroxymonosulfate/LaCoO3 system for tetracycline degradation: Performance and effects of co-existing inorganic anions and natural organic matter. Journal of Water Process Engineering, 2021, 43, 102231.	2.6	27
167	Insights into the removal of Cr(VI) by a biochar–iron composite from aqueous solution: Reactivity, kinetics and mechanism. Environmental Technology and Innovation, 2021, 24, 102057.	3.0	27
168	Study of Herbicide Alachlor Removal in a Photocatalytic Process through the Examination of the Reaction Mechanism. Industrial & Engineering Chemistry Research, 2004, 43, 5027-5031.	1.8	26
169	Enhancement of ozone oxidation and its associated processes in the presence of surfactant: Degradation of atrazine. Chemosphere, 2006, 64, 931-936.	4.2	26
170	Removal of Simazine in a UV/TiO ₂ Heterogeneous System. Journal of Agricultural and Food Chemistry, 2009, 57, 6944-6949.	2.4	26
171	The mechanism study of efficient degradation of hydrophobic nonylphenol in solution by a chemical-free technology of sonophotolysis. Journal of Hazardous Materials, 2016, 308, 386-393.	6.5	26
172	Formation of multi-layered chitosan honeycomb spheres via breath-figure-like approach in combination with co-precipitation processing. Materials Letters, 2018, 211, 91-95.	1.3	26
173	Degradation of Triclosan by Recyclable MnFe ₂ O ₄ -Activated PMS: Process Modification for Reduced Toxicity and Enhanced Performance. Industrial & Engineering Chemistry Research, 2020, 59, 4257-4264.	1.8	26
174	A new insight on enhanced Pb(II) removal by sludge biochar catalyst coupling with ultrasound irradiation and its synergism with phenol removal. Chemosphere, 2021, 263, 128287.	4.2	26
175	The direct and indirect photolysis of 4,4′-dichlorobiphenyl in various surfactant/solvent-aided systems. Water Research, 2002, 36, 2187-2194.	5.3	25
176	In situ co-precipitation preparation of a superparamagnetic graphene oxide/Fe3O4 nanocomposite as an adsorbent for wastewater purification: synthesis, characterization, kinetics, and isotherm studies. Environmental Science and Pollution Research, 2018, 25, 17310-17320.	2.7	25
177	Efficient degradation of bisphenol A using High-Frequency Ultrasound: Analysis of influencing factors and mechanistic investigation. Journal of Cleaner Production, 2019, 232, 1195-1203.	4.6	25
178	Model Applications and Intermediates Quantification of Atrazine Degradation by UV-Enhanced Fenton Process. Journal of Agricultural and Food Chemistry, 2006, 54, 1804-1813.	2.4	24
179	Permanganate with a double-edge role in photodegradation of sulfamethoxazole: Kinetic, reaction mechanism and toxicity. Chemosphere, 2018, 191, 494-502.	4.2	24
180	Utilization of photochemical circulation between NO3â^' and NO2â^' in water to degrade photoinert dimethyl phthalate: Influence of organic media and mechanism study. Applied Catalysis B: Environmental, 2019, 259, 117958.	10.8	24

Wеі Сни

#	Article	IF	CITATIONS
181	Improved Catalytic Performance of Ethane Dehydrogenation in the Presence of CO ₂ over Zr-Promoted Cr/SiO ₂ . ACS Omega, 2019, 4, 22562-22573.	1.6	24
182	Synthesis of copper oxide vegetable sponges and their antibacterial, electrochemical and photocatalytic performance. Journal of Materials Science, 2011, 46, 2179-2184.	1.7	23
183	Novel synthesis of RGO/NiCoAl–LDH nanosheets on nickel foam for supercapacitors with high capacitance. RSC Advances, 2016, 6, 113123-113131.	1.7	23
184	Reduction removal of hexavalent chromium by zinc-substituted magnetite coupled with aqueous Fe(II) at neutral pH value. Journal of Colloid and Interface Science, 2017, 500, 20-29.	5.0	23
185	Exploring a broadened operating pH range for norfloxacin removal via simulated solar-light-mediated Bi2WO6 process. Chinese Journal of Catalysis, 2019, 40, 673-680.	6.9	23
186	One-step plasma-enabled catalytic carbon dioxide hydrogenation to higher hydrocarbons: significance of catalyst-bed configuration. Green Chemistry, 2021, 23, 1642-1647.	4.6	23
187	The study of lag phase and rate improvement of TCE decay in UV/surfactant systems. Chemosphere, 2000, 41, 1199-1204.	4.2	22
188	Selection of Supported Cobalt Substrates in the Presence of Oxone for the Oxidation of Monuron. Journal of Agricultural and Food Chemistry, 2007, 55, 5708-5713.	2.4	22
189	Catalytic synthesis of 2-methylpyrazine over Cr-promoted copper based catalyst via a cyclo-dehydrogenation reaction route. Journal of Chemical Sciences, 2010, 122, 621-630.	0.7	22
190	Degradation of linuron by UV, ozonation, and UV/O3 processes—Effect of anions and reaction mechanism. Journal of Hazardous Materials, 2010, 180, 514-523.	6.5	22
191	Surface Modification of Bituminous Coal and Its Effects on Methane Adsorption. Chinese Journal of Chemistry, 2013, 31, 1102-1108.	2.6	22
192	Insights into peroxymonosulfate activation for carbofuran degradation under visible LED via a double-component photocatalyst of Fe (III) impregnated N-doped TiO2. Chemosphere, 2019, 237, 124487.	4.2	22
193	Mesoporous Face-Centered-Cubic In ₄ Ni Alloy Nanorices: Superior Catalysts for Hydrazine Dehydrogenation in Aqueous Solution. ACS Applied Materials & Interfaces, 2016, 8, 25268-25278.	4.0	21
194	Synchronous removal of Cr(VI) and phosphates by a novel crayfish shell biochar-Fe composite from aqueous solution: Reactivity and mechanism. Journal of Environmental Chemical Engineering, 2022, 10, 107396.	3.3	21
195	Photodegradation mechanism and rate improvement of chlorinated aromatic dye in non-ionic surfactant solutions. Water Research, 2001, 35, 2453-2459.	5.3	20
196	A disappearance model for the prediction of trichlorophenol ozonation. Chemosphere, 2003, 51, 289-294.	4.2	20
197	Cutting Of Carbon Nanotubes Via Solution Plasma Processing. Plasma Chemistry and Plasma Processing, 2010, 30, 897-905.	1.1	20
198	Application of Fourier transform ion cyclotron resonance mass spectrometry in deciphering molecular composition of soil organic matter: A review. Science of the Total Environment, 2021, 756, 144140	3.9	20

#	Article	IF	CITATIONS
199	Atrazine removal by catalytic oxidation processes with or without UV irradiation. Applied Catalysis B: Environmental, 2005, 58, 157-163.	10.8	19
200	Photo-oxidation of o-chloroaniline in the presence of TiO2 and IO3â^': A study of photo-intermediates and successive IO3â^' dose. Chemical Engineering Journal, 2008, 136, 180-187.	6.6	19
201	Photo-assisted degradation of 2,4,5-trichlorophenol by Electro-Fe(II)/Oxone® process using a sacrificial iron anode: Performance optimization and reaction mechanism. Chemical Engineering Journal, 2013, 215-216, 643-650.	6.6	19
202	Insights into key parameters of MnO2 catalyst toward high catalytic combustion performance. Journal of Materials Science, 2021, 56, 6361-6373.	1.7	19
203	g–C3N4 induced acceleration of Fe3+/Fe2+ cycles for enhancing metronidazole degradation in Fe3+/peroxymonosulfate process under visible light. Chemosphere, 2022, 293, 133611.	4.2	19
204	Modeling the ozonation of herbicide 2,4-D through a kinetic approach. Chemosphere, 2004, 55, 647-652.	4.2	18
205	Effects of nonaqueous phase liquids on the washing of soil in the presence of nonionic surfactants. Water Research, 2005, 39, 340-348.	5.3	18
206	Catalytic Chemical Vapor Deposition of Methane to Carbon Nanotubes: Copper Promoted Effect of Ni/MgO Catalysts. Journal of Nanotechnology, 2014, 2014, 1-5.	1.5	18
207	Electrochemical oxidation of guaiacol to increase its biodegradability or just remove COD in terms of anodes and electrolytes. RSC Advances, 2016, 6, 4858-4866.	1.7	18
208	Synergetic Bimetallic NiCo/CNT Catalyst for Hydrogen Production by Glycerol Steam Reforming: Effects of Metal Species Distribution. Industrial & Engineering Chemistry Research, 2020, 59, 17259-17268.	1.8	18
209	Diphenamid photodegradation using Fe(III) impregnated N-doped TiO2/sulfite/visible LED process: Influence of wastewater matrix, kinetic modeling, and toxicity evaluation. Chemosphere, 2020, 256, 127094.	4.2	18
210	Influence of Zirconia Promoter on Catalytic Properties of Cu–Cr–Si Catalysts for Methanol Synthesis at High CO Conversion in Slurry Phase. Catalysis Letters, 2006, 108, 113-118.	1.4	17
211	Glow Discharge Plasma-Assisted Preparation of Nickel-Based Catalyst for Carbon Dioxide Reforming of Methane. Chinese Journal of Chemical Physics, 2008, 21, 481-486.	0.6	17
212	Simulation and quantification of the natural decay of a typical endocrine disrupting chemical Atrazine in an aquatic system. Journal of Hazardous Materials, 2011, 192, 1260-1266.	6.5	17
213	Non-thermal plasma-treated gold catalyst for CO oxidation. RSC Advances, 2014, 4, 25729-25735.	1.7	17
214	Triclosan removal by heterogeneous Fenton-like process: Studying the kinetics and surface chemistry of Fe3O4 as catalyst. Journal of Environmental Chemical Engineering, 2019, 7, 103432.	3.3	17
215	Optimizing the removal of nitrate from aqueous solutions via reduced graphite oxide–supported nZVI: synthesis, characterization, kinetics, and reduction mechanism. Environmental Science and Pollution Research, 2019, 26, 3932-3945.	2.7	17
216	Variations of disinfection byproduct precursors through conventional drinking water treatment processes and a real-time monitoring method. Chemosphere, 2021, 272, 129930.	4.2	17

#	Article	IF	CITATIONS
217	Upgrading the conventional grease trap using a tube settler. Environment International, 2000, 26, 17-22.	4.8	16
218	The mechanisms of rate enhancing and quenching of trichloroethene photodecay in the presence of sensitizer and hydrogen sources. Water Research, 2002, 36, 2525-2532.	5.3	16
219	Ozonation of endocrine disrupting chemical BHA under the suppression effect by salt additive—With and without H2O2. Journal of Hazardous Materials, 2007, 144, 249-254.	6.5	16
220	Doping effects of manganese on the catalytic performance and structure of NiMgO catalysts for controllabe synthesis of multi-walled carbon nanotubes. Journal of Energy Chemistry, 2014, 23, 781-788.	7.1	16
221	Effect of Ca modification on the catalytic performance of Ni/AC for CO2methanation. Integrated Ferroelectrics, 2016, 172, 40-48.	0.3	16
222	Catalytic ozonation of sulfamethoxazole by composite iron-manganese silicate oxide: cooperation mechanism between adsorption and catalytic reaction. Environmental Science and Pollution Research, 2016, 23, 21360-21368.	2.7	16
223	Synthesis of Cu–Co Catalysts for Methanol Decomposition to Hydrogen Production via Deposition–Precipitation with Urea Method. Catalysis Letters, 2019, 149, 2671-2682.	1.4	16
224	Enhanced degradation of metronidazole by cobalt doped TiO2/sulfite process under visible light. Separation and Purification Technology, 2022, 291, 120900.	3.9	16
225	Converting Poisonous Sulfate Species to an Active Promoter on TiO ₂ Predecorated MnO _{<i>x</i>} Catalysts for the NH ₃ -SCR Reaction. ACS Applied Materials & Interfaces, 2021, 13, 61237-61247.	4.0	16
226	The modelling of trichloroethene photodegradation in Brij 35 surfactant by two-stage reaction. Chemosphere, 2001, 44, 211-215.	4.2	15
227	The partitioning and modelling of pesticide parathion in a surfactant-assisted soil-washing system. Chemosphere, 2006, 64, 711-716.	4.2	15
228	Synthesis of 2-Methylpyrazine Over Highly Dispersed Copper Catalysts. Catalysis Letters, 2012, 142, 492-500.	1.4	15
229	Monodisperse amorphous CuB ₂₃ alloy short nanotubes: novel efficient catalysts for Heck coupling of inactivated alkyl halides and alkenes. RSC Advances, 2014, 4, 45838-45843.	1.7	15
230	Layered Double Hydroxides Derived <scp>ZnOâ€Al₂O₃</scp> Supported Pdâ€Ag Catalysts for Selective Hydrogenation of Acetylene. Chinese Journal of Chemistry, 2017, 35, 1009-1015.	2.6	15
231	Modeling the sequential photodechlorination of hexachlorobenzene in surfactant micelles. Water Research, 2002, 36, 843-850.	5.3	14
232	Removal of phenylurea herbicide monuron via riboflavin-mediated photosensitization. Chemosphere, 2007, 69, 177-183.	4.2	14
233	Keggin-type H4PVMo11O40-based catalysts for the isobutane selective oxidation. Science China Chemistry, 2010, 53, 2039-2046.	4.2	14
234	Visible Light-Induced Photodegradation of Simazine in Aqueous TiO ₂ Suspension. Industrial & Engineering Chemistry Research, 2013, 52, 13580-13586.	1.8	14

Wеі Сни

#	Article	IF	CITATIONS
235	Enhancement of UV-assisted TiO2 degradation of ibuprofen using Fenton hybrid process at circumneutral pH. Chinese Journal of Catalysis, 2018, 39, 701-709.	6.9	14
236	Confined PtNi catalysts for enhanced catalytic performances in one-pot cellobiose conversion to hexitols: a combined experimental and DFT study. Green Chemistry, 2019, 21, 5999-6011.	4.6	14
237	Remarkable effect of Co substitution in magnetite on the reduction removal of Cr(VI) coupled with aqueous Fe(II): Improvement mechanism and Cr fate. Science of the Total Environment, 2019, 656, 400-408.	3.9	14
238	Bisphenol S degradation via persulfate activation under UV-LED using mixed catalysts: Synergistic effect of Cu–TiO2 and Zn–TiO2 for catalysis. Chemosphere, 2022, 286, 131797.	4.2	14
239	Effects of uvâ€decolouring of aromatic dyes with different chemical structures. Toxicological and Environmental Chemistry, 1997, 63, 247-255.	0.6	13
240	Photoreductive Model of Disperse Orange 11 in Aqueous Acetone and Triethylamine. Journal of Environmental Engineering, ASCE, 2001, 127, 741-747.	0.7	13
241	Semiconductor-Catalyzed Photodegradation ofo-Chloroaniline:Â Products Study and Iodate Effect. Industrial & Engineering Chemistry Research, 2007, 46, 4740-4746.	1.8	13
242	Ligand Size Effect on PdL <i>n</i> Oxidative Addition with Aryl Bromide: A DFT Study. Chinese Journal of Chemical Physics, 2010, 23, 175-179.	0.6	13
243	A Study of CO ₂ Methanation over Ni-Based Catalysts Supported by CNTs with Various Textural Characteristics. International Journal of Chemical Engineering, 2015, 2015, 1-7.	1.4	13
244	Highly stable bimetallic Au–Cu supported on Al ₂ O ₃ for selective CO oxidation in H ₂ -rich gas: effects of Cu/Au atomic ratio and sensitive influence of particle size. RSC Advances, 2016, 6, 4899-4907.	1.7	13
245	The system design of atrazine oxidation by catalytic oxidation process through a kinetic approach. Water Research, 2003, 37, 3997-4003.	5.3	12
246	The photocatalyic degradation and modeling of 2,4-Dichlorophenoxyacetic acid by bismuth tungstate/peroxide. Chemical Engineering Journal, 2013, 223, 665-669.	6.6	12
247	Anchoring and promotion effects of metal oxides on silica supported catalytic gold nanoparticles. Journal of Colloid and Interface Science, 2016, 482, 135-141.	5.0	12
248	Heterogeneous Catalytic Ozonation of Sulfamethoxazole in Aqueous Solution over Composite Iron–Manganese Silicate Oxide. Ozone: Science and Engineering, 2017, 39, 24-32.	1.4	12
249	Improvement of zinc substitution in the reactivity of magnetite coupled with aqueous Fe(II) towards nitrobenzene reduction. Journal of Colloid and Interface Science, 2018, 517, 104-112.	5.0	12
250	ZIF-67 Derived Hollow Structured Co3O4 Nanocatalysts: Tunable Synthetic Strategy Induced Enhanced Catalytic Performance. Catalysis Letters, 2019, 149, 3058-3065.	1.4	12
251	Two-dimensional layered carbon-based catalytic ozonation for water purification: Rational design of catalysts and an in-depth understanding of the interfacial reaction mechanism. Science of the Total Environment, 2022, 832, 155071.	3.9	12
252	The system design of UV-assisted catalytic oxidation process––degradation of 2,4-D. Chemosphere, 2004, 57, 171-178.	4.2	11

#	Article	IF	CITATIONS
253	Preparation of the supported heteropolyacids catalyst by ultrasound-plasma treatment. Journal Wuhan University of Technology, Materials Science Edition, 2008, 23, 234-238.	0.4	11
254	Effects of glow discharge plasma on Cu–Co–Al-based supported catalysts for higher alcohol synthesis. Reaction Kinetics and Catalysis Letters, 2009, 97, 243-247.	0.6	11
255	The Photodegradation and Modeling of a Typical NAPL, Trichloroethene, by Monochromatic UV Irradiations. Environmental Science & Technology, 2009, 43, 1455-1459.	4.6	11
256	Enhanced Conversion of Cellobiose to Sugar Alcohols by Controlled Dispersion of Ruthenium Nanoparticles Inside Carbon Nanotube Channels. Catalysis Letters, 2013, 143, 1139-1144.	1.4	11
257	Li ₉ V ₃ (P ₂ O ₇) ₃ (PO ₄) ₂ nanotubes fabricated by a simple molten salt approach with excellent cycling stability and enhanced rate capability in lithium-ion batteries. RSC Advances, 2015, 5, 243-247.	1.7	11
258	Reaction Mechanism of Photoreduction of 2,4-Dichlorophenoxyacetic Acid in Surfactant Micelles. Industrial & Engineering Chemistry Research, 2005, 44, 1645-1651.	1.8	10
259	Plasma assisted preparation of cobalt catalysts by sol–gel method for methane combustion. Journal of Sol-Gel Science and Technology, 2008, 47, 354-359.	1.1	10
260	The photodegradation of trichloroethylene with or without the NAPL by UV irradiation in surfactant solutions. Journal of Hazardous Materials, 2009, 161, 196-201.	6.5	10
261	Novel F–V2O5/SiO2 catalysts for oxidative dehydrogenation of propane. Reaction Kinetics, Mechanisms and Catalysis, 2010, 101, 141-151.	0.8	10
262	Nanoparticles-in-concavities as efficient nanocatalysts for carbon dioxide reforming of methane to hydrogen and syngas. Catalysis Science and Technology, 2016, 6, 4565-4576.	2.1	10
263	Toward Computational Design of Catalysts for CO ₂ Selective Reduction via Reaction Phase Diagram Analysis. Advanced Theory and Simulations, 2019, 2, 1800200.	1.3	10
264	Facile Fabrication of Nickel Aluminum Layered Double Hydroxide/Carbon Nanotube Electrodes Toward High-Performance Supercapacitors. ACS Omega, 2020, 5, 24693-24699.	1.6	10
265	Microemulsion solventing-out co-precipitation strategy for fabricating highly active Cu–ZnO/Al2O3 dual site catalysts for reverse water gas shift. Catalysis Science and Technology, 2020, 10, 2343-2352.	2.1	10
266	Photocatalysis of naphthalene by Fe3O4/Oxone/UV: Simultaneous radical and non-radical pathways. Journal of Environmental Chemical Engineering, 2021, 9, 105076.	3.3	10
267	Reactor design and kinetics study of 4,4′-dichlorobiphenyl photodecay in surfactant solution by using a photosensitizer and hydrogen source. Water Research, 2003, 37, 2442-2448.	5.3	9
268	Riboflavin-sensitized photooxidation of phenylurea herbicide monuron in aqueous peroxide solution. Chemical Engineering Journal, 2009, 152, 103-109.	6.6	9
269	Immobilization of 12-phosphotungstic heteropolyacid on amine-functionalized SiO2 for tetrahydrofuran polymerization. Science Bulletin, 2010, 55, 2652-2656.	1.7	9
270	Nano Ru catalysts supported on carbon nanotubes for cellobiose conversion to sugar alcohols: effects of CNT channel size. RSC Advances, 2015, 5, 103669-103673.	1.7	9

#	Article	IF	CITATIONS
271	Atmospheric Discharge Plasma Enhanced Preparation of Pd/TiO2 Catalysts for Acetylene Selective Hydrogenation. Topics in Catalysis, 2017, 60, 1009-1015.	1.3	9
272	Synthesis of graphene-like CuB23 nanosheets with a fast and stable response to H2S at ppb detection levels. Journal of Materials Chemistry C, 2017, 5, 3216-3221.	2.7	9
273	Effect of Plasma Treatment on Cobalt–Boron Catalytic Activity for Hydrogen Generation from Alkali NaBH4 Solution. Plasma Chemistry and Plasma Processing, 2010, 30, 663-677.	1.1	8
274	Contribution of Ash Content Related to Methane Adsorption Behaviors of Bituminous Coals. International Journal of Chemical Engineering, 2014, 2014, 1-11.	1.4	8
275	Photo-oxidation of an endocrine disrupting chemical o-chloroaniline with the assistance of TiO2 and iodate: Reaction parameters and kinetic models. Chemical Engineering Journal, 2014, 248, 273-279.	6.6	8
276	Sonochemical synthesis of magnetic properties of Fe ₃ O ₄ /CNT nanocomposites. Integrated Ferroelectrics, 2017, 179, 77-83.	0.3	8
277	Chitosan-Derived Porous N-Doped Carbon as a Promising Support for Ru Catalysts in One-Pot Conversion of Cellobiose to Hexitol. ACS Sustainable Chemistry and Engineering, 2021, 9, 12655-12662.	3.2	8
278	A Quantitative Structure—Activity Relationship for Solubilization of Nonpolar Compounds by Nonionic Surfactant Micelles. ACS Symposium Series, 1995, , 24-37.	0.5	7
279	Enhancement of hydrogen sorption on metal(Ni, Rh, Pd) functionalized carbon nanotubes: a DFT study. Chemical Research in Chinese Universities, 2017, 33, 422-429.	1.3	7
280	Tuning Interfacial Electron Transfer by Anchoring NiFe-LDH on In-situ Grown Cu2O for Enhancing Oxygen Evolution. Catalysis Letters, 2020, 150, 3049-3057.	1.4	7
281	Degradation of 1-naphthylamine by a UV enhanced Fe2+/peroxymonosulfate system: A novel pH-dependent activation pathway. Chemical Engineering Journal, 2022, 443, 136299.	6.6	7
282	Pollution source identification and waste loading reduction at Chinese fast food restaurants. Environment International, 1999, 25, 97-107.	4.8	6
283	The rate improvement and modeling of trichloroethene photodegradation by acetone sensitizer in surfactant solution. Chemosphere, 2001, 44, 943-947.	4.2	6
284	Photocatalytic degradation of dye pollutants in the presence of acetone. Water Science and Technology, 2001, 44, 173-180.	1.2	6
285	Comprehensive Study of the Wavelength Effect on Oxidation Processes of 2-Chloroaniline. Industrial & Engineering Chemistry Research, 2006, 45, 3769-3775.	1.8	6
286	Effect of ferrioxalate-exchanged resin on the removal of 2,4-D by a photocatalytic process. Journal of Molecular Catalysis A, 2006, 255, 236-242.	4.8	6
287	Cooperation of Fe(II) and peroxymonosulfate for enhancement of sulfamethoxazole photodegradation: mechanism study and toxicity elimination. RSC Advances, 2020, 10, 35646-35657.	1.7	6
288	Toward a comparative description between transition metal and zeolite catalysts for methanol conversion. Physical Chemistry Chemical Physics, 2020, 22, 5293-5300.	1.3	6

#	Article	IF	CITATIONS
289	Unveiling the Origin of Alkali Metal (Na, K, Rb, and Cs) Promotion in CO2 Dissociation over Mo2C Catalysts. Materials, 2022, 15, 3775.	1.3	6
290	Photooxidation of 2,4-dichlorophenoxyacetic acid by ferrous oxalate-mediated system. Water Science and Technology, 2004, 49, 117-122.	1.2	5
291	Comparative Study of Textural Characteristics on Methane Adsorption for Carbon Spheres Produced by CO ₂ Activation. International Journal of Chemical Engineering, 2014, 2014, 1-7.	1.4	5
292	Investigation on the Kinetics of Heterogeneous Catalytic Ozone Decomposition in Aqueous Solution over Composite Iron-Manganese Silicate Oxide. Ozone: Science and Engineering, 2016, 38, 434-442.	1.4	5
293	Assembling Carbon into Anatase TiO2 as Interstitial Atoms towards Photocatalytic Activity. European Journal of Inorganic Chemistry, 2018, 2018, 4370-4374.	1.0	5
294	A periodic density functional theory study of adsorption of CO ₂ on anorthite (001) surface and effect of water. Journal of Theoretical and Computational Chemistry, 2019, 18, 1950010.	1.8	5
295	A comparative study on phenazone degradation by sulfate radicals based processes. Environmental Research, 2020, 191, 110054.	3.7	5
296	Amphoteric Effect of Humic Acids in Surfactant-Aided Photolysis of Polychlorobiphenyls. Journal of Environmental Engineering, ASCE, 2003, 129, 716-722.	0.7	4
297	Transformation of 2,4-dichlorophenoxy-ethanoic acid(2,4-D) by a photoassisted ferrous oxalate/H2O2 system. Journal of Chemical Technology and Biotechnology, 2004, 79, 663-669.	1.6	4
298	Hybrid System to Upgrade Conventional Fenton's Process by Incorporating Photo-Fenton as A Successive Treatment Process:  Degradation of Monuron. Industrial & Engineering Chemistry Research, 2007, 46, 1505-1510.	1.8	4
299	The role of oxalate in the kinetics of 2,4-D oxidation over ferrous ion-supported catalysts. Journal of Molecular Catalysis A, 2007, 274, 50-57.	4.8	4
300	Photochemical Degradation of 2,4,6-Trichlorophenol in the Brij 35 Micellar Solution: pH Control on Product Distribution. Industrial & Engineering Chemistry Research, 2009, 48, 10211-10216.	1.8	4
301	CuZnAl mixed-metal oxides prepared by a novel sol–gel route and the application for synthesis of 2- methylpyrazine. Journal of Sol-Gel Science and Technology, 2011, 58, 142-147.	1.1	4
302	Strategy for enhanced performance of silicon nanoparticle anodes for lithium-ion batteries. RSC Advances, 2022, 12, 17889-17897.	1.7	4
303	Oxone activated TiO2 in presence of UV-LED light for the degradation of moxifloxacin: A mechanistic study. Arabian Journal of Chemistry, 2022, 15, 104061.	2.3	4
304	Photochemical Degradation of 2,4,6-Trichlorophenol in the Presence of a Nonionic Surfactant: pH Control on Reaction Kinetics. Journal of Environmental Engineering, ASCE, 2007, 133, 641-645.	0.7	3
305	Calcium Salts of Tungstophoric Acid Supported on Silica as Novel Catalysts for Tetrahydrofuran Polymerization. Catalysis Letters, 2011, 141, 1670-1676.	1.4	3
306	Highly Efficient SiC-Supported Ni-Based Catalysts with Enhanced Recycle Stability for One-Pot Cellobiose Hydrolytic Hydrogenation to Hexitols. ACS Sustainable Chemistry and Engineering, 0, , .	3.2	3

#	ARTICLE	IF	CITATIONS
307	Microwave-assisted hydrothermal synthesis of lithium-rich layered oxide cathode materials with high stability. Ionics, 2020, 26, 6013-6022.	1.2	3
308	Advances in Heterocatalysis by Nanomaterials. Nanomaterials, 2020, 10, 609.	1.9	3
309	Reactor Design and Modeling of the Fe(II)-Catalyzed Oxidation of Trichlorophenol. Industrial & Engineering Chemistry Research, 2004, 43, 6797-6802.	1.8	2
310	Effect of Thermal Treatment on Structure and Catalytic Activity of Supported Fischer-Tropsch Nano-Cobalt Catalysts for Clean Fuels. Chinese Journal of Chemical Physics, 2007, 20, 743-747.	0.6	2
311	Effects of potassium on MgO-supported Fe-Mn catalysts for the hydrogenation of carbon monoxide to light alkenes. Reaction Kinetics and Catalysis Letters, 2008, 94, 139-147.	0.6	2
312	Influences of pore size on production of 2-methylpyrazine over bifunctional CuO/ZnO/meso-SiO2 catalysts. Research on Chemical Intermediates, 2013, 39, 1301-1311.	1.3	2
313	Promoting Effect of Ce Doping on the CuZn/ZnAl2O4 Catalysts for Methanol Decomposition to Hydrogen and Carbon Monoxide. Catalysis Letters, 2022, 152, 1109-1118.	1.4	2
314	The study of rate improvement of trichloroethene (TCE) decay in UV system with hydrogen source. Water Science and Technology, 2001, 44, 27-33.	1.2	1
315	Heterogeneous Photocatalytic Oxidation of o-Chloroaniline Immobilizing on Recyclable TiO2. Industrial & Engineering Chemistry Research, 2008, 47, 7564-7569.	1.8	1
316	Enhanced heterogenous hydration of SO 2 through immobilization of pyridinic-N on carbon materials. Royal Society Open Science, 2020, 7, 192248.	1.1	1
317	Impacts of Mo Promotion on Nickel-Based Catalysts for the Synthesis of High Quality Carbon Nanotubes Using CO ₂ as the Carbon Source. Journal of Nanoscience and Nanotechnology, 2020, 20, 1109-1117.	0.9	1
318	Effects of Humic Materials on Photodegradation of Chlorinated Aromatic Dye in Surfactant Solution. Journal of Environmental Engineering, ASCE, 2003, 129, 500-505.	0.7	0
319	Reply to the comment of "the mechanisms of rate enhancing and quenching of trichloroethene photodecay in the presence of sensitizer and hydrogen sources― Water Research, 2004, 38, 2793-2794.	5.3	0
320	Effect of Fe content on FeMn catalysts for light alkenes synthesis. Frontiers of Chemical Engineering in China, 2008, 2, 315-318.	0.6	0
321	Reactor model development: The removal performance of ferrous-catalysed photo-oxidation process by examining the reaction parameters. Journal of Hazardous Materials, 2009, 167, 199-204.	6.5	0
322	Nano-porous Composites Based on Heteropolyacid Functionalized Ionic Liquid: Synthesis, Characterization, and Catalytic Performance in Esterification. Chinese Journal of Chemical Physics, 2010, 23, 473-478.	0.6	0
323	Insight into Adsorption of C ₂ H ₂ and H ₂ on Doped Graphene with Nonmetallic Atom (N, P, S): A Density Functional Theory Study. Journal of Nanoscience and Nanotechnology, 2020, 20, 1288-1295.	0.9	0